Experimental studies of labyrinthine instabilities of miscible ferrofluids in a Hele-Shaw cell

C.-Y. Wen, Ching-Yao Chen, and D.-C. Kuan

Citation: Physics of Fluids (1994-present) **19**, 084101 (2007); doi: 10.1063/1.2756083
View online: http://dx.doi.org/10.1063/1.2756083
View Table of Contents: http://scitation.aip.org/content/aip/journal/pof2/19/8?ver=pdfcov
Published by the AIP Publishing

Experimental studies of labyrinthine instabilities of miscible ferrofluids in a Hele-Shaw cell

C.-Y. Wen
Department of Aeronautics and Astronautics, National Cheng-Kung University, Tainan, Taiwan, Republic of China

Ching-Yao Chen[a)]
Department of Mechanical Engineering, National Chiao Tung University, Hsinchu, Taiwan, Republic of China

D.-C. Kuan
Department of Mechanical and Automation Engineering, Da-Yeh University, Chang-Hwa, Taiwan, Republic of China

(Received 1 February 2007; accepted 30 May 2007; published online 3 August 2007)

The first systematic experimental studies on the labyrinthine instabilities of miscible ferrofluids in a Hele-Shaw cell are presented. Two distinct features of instabilities are observed: (i) the miscible labyrinthine fingers caused by the magnetic dipolar forces; (ii) the secondary waves dominated by the third-dimensional effects. Prominence of the labyrinthine fingers is confirmed to be affected significantly by both the magnetic field strength and the cell gap width. On the other hand, wave selection of the secondary wave numbers is mainly dominated by the gap width. The characteristic wavelength λ of the secondary waves follows a nearly linear correlation with the gap width h, which is consistent with earlier findings on the viscous fingering instability. The wavelength can be approximated as $\lambda \approx (7 \pm 1)h$. © *2007 American Institute of Physics*. [DOI: 10.1063/1.2756083]

I. INTRODUCTION AND EXPERIMENTAL SETUP

A. Introduction

Ferrofluids are colloidal fluids with magnetic particles suspended in nonmagnetic carrier fluids. These magnetic fluids have both the fluidity of liquids and the magnetic properties of solids, making them a fascinating field of research for physicists, chemists, and engineers.[1,2] Their pronounced superparamagnetic behavior can be applied to manipulate their flow and interfacial behaviors using external magnetic fields. Consequently, the patterns of interfacial instabilities in ferrofluids have been investigated intensively. A more detailed review regarding the recent development of interfacial instabilities in ferrofluids is presented in Chen *et al.*[3] One type of remarkable pattern is associated with the so-called labyrinthine instability, where highly branched structures are formed when a ferrofluid drop is confined in a Hele-Shaw cell and subjected to a perpendicular external field.[1–20] Even with the rich physics and the great variety of situations in the study of labyrinthine instability in ferrofluids, most of the investigations focus on an immiscible interface, in which ferrofluids establish a well defined and sharp interface without mixing with the surrounding nonmagnetic fluids. Detailed mechanisms of labyrinthine instability on the immiscible interfaces, such as effects of the dimensionless magnetic Bond number B_o ($B_o \equiv 2M^2h/\sigma$) and the dimensionless diameter $p(p \equiv d/h)$, that characterize the ratio of magnetic force to the surface tension and the ratio of droplet diameter d to the cell gap width h, respectively, have been well addressed both theoretically and experimentally.[1,4–8,10–14] Here, the notations of M and σ represent the magnetization and the surface tension of the magnetic fluids against the surrounding fluids.

On the other hand, it is also important and interesting to understand the similar labyrinthine instability in a miscible interface, where the conventional interfacial tension is not considered and the diffusive effect takes over instead. Even though the development of the labyrinthine instability in miscible ferrofluids has been first investigated by qualitative experiments more than two decades ago,[15] only quite recently a more systematic theoretical analysis[17] and intensive numerical simulations[16,18–20] have been reported. The above studies indicate that, instead of the magnetic Bond number, the miscible labyrinthine instability involves the effect of diffusion, which is represented by a dimensionless magnetic Peclet number Pe ($\mathrm{Pe} \equiv M^2d^2/\eta D$) (Refs. 16 and 18) or its equivalent.[17] The notations D and η stand for the diffusion coefficient and viscosity. Igonin and Cebers[17] present linear stability analysis for both a sharp interface and a diffused interface, respectively, and establish a parallel between approaches based on Darcy's law and on the Brinkman equations. Relevant results, such as the wave numbers, growth rates, and the most dangerous modes, are predicted. As for the computer simulations, a series of numerical simulations by schemes of high order of accuracy have extended the study of the miscible ferrofluid problems in many ways, considering the actions of perpendicular and azimuthal magnetic fields in radial and rotating Hele-Shaw cells.[16,18–20] The simulations reveal intensive fingerings and analyze the prominence of fingers for various control parameters, including the magnetic Peclet number, the viscosity contrast and

[a)]Author to whom correspondence should be addressed. Electronic mail: chingyao@mail.nctu.edu.tw

different convective effects. In addition, studies in the microconvective instability by an applied field are also recently reported,[21] in which the dimensionless diffusive and Rayleigh numbers are calculated both from experiments and linear stability analysis. However, these studies are not as complete as the thorough investigations in the immiscible situations. The reason is mainly the diffusive feature of miscible ferrofluids. It has been confirmed that the stability depends significantly on the initial concentration gradient as well as the local viscosity of the mixing interface.[16–19] In contrast to the homogeneous fields of viscosity and magnetization in a well defined immiscible domain, the diffusive effects lead to transient and nonuniform distributions of viscosity and magnetization in the mixing region of miscible fluids. These time-dependent and inhomogeneous distributions cause significant difficulties in resolving the flow fields theoretically, as well as properly establishing experimental setups. Lacking the experimental investigations, the theoretical models as well as the numerical simulations based on them are not able to be verified. As a result, detailed and systematically experimental results would be very desirable. These experiments would not just provide more insights of the interesting interfacial phenomena, but could also validate the early theoretical and simulating results either based on Darcy's law or the Brinkman equations.

Another interesting issue concerning the interfacial instability on a miscible interface in a Hele-Shaw cell is the wavelength selection. For a sufficiently high Peclet number (Pe) or Rayleigh number (Ra), i.e., $\mathrm{Pe},\mathrm{Ra} > O(10^2)$, strong dependencies between the wave number (or wavelength) and the gap width have been reported for viscous fingering instability in various flow situations.[17,22–27] Under these conditions, the conventional Hele-Shaw equations which apply the averaging velocities across the gap cannot describe the complete instability phenomena. In order to accurately resolve the complete interfacial evolution, solutions of the full three-dimensional Stokes equations or Brinkman equations are required,[17,24–27] referred to as the Stokes regime. It has also been found that in general the wavelength λ of miscible fingers correlates nearly linearly to the gap width h in this Stokes regime. The wavelength λ is measured experimentally as $\lambda \approx 4h$ in a radial displacement,[22] in which a source flow of less viscous fluids is placed at the origin of the cell and displaces the surrounding viscous fluids outwardly. In the situation of a downward displacement[23] which a lighter and less viscous fluid flow is introduced from the top in a vertical Hele-Shaw configuration, a correlation of $\lambda \approx (5 \pm 1)h$ is observed. For a gravity-driven flow, $\lambda \approx 2.3h$ is obtained by an analytical study,[24] which agrees closely with the experimental result of $\lambda \approx (5 \pm 1)h$.[25] On the other hand, in the situations of a low Peclet number or Rayleigh number $[\mathrm{Pe},\mathrm{Ra} < O(10^2)]$, dispersion across the gap is significant. The conventional Hele-Shaw model is sufficient to resolve the interfacial instability. It is referred to as the Hele-Shaw regime. Thus, it would also be interesting to experimentally investigate the gap influence to miscible labyrinthine instability in a similar Hele-Shaw configuration. It is noteworthy that similar gap influence to miscible magnetic fluids has been confirmed theoretically by thorough linear stability analysis.[17]

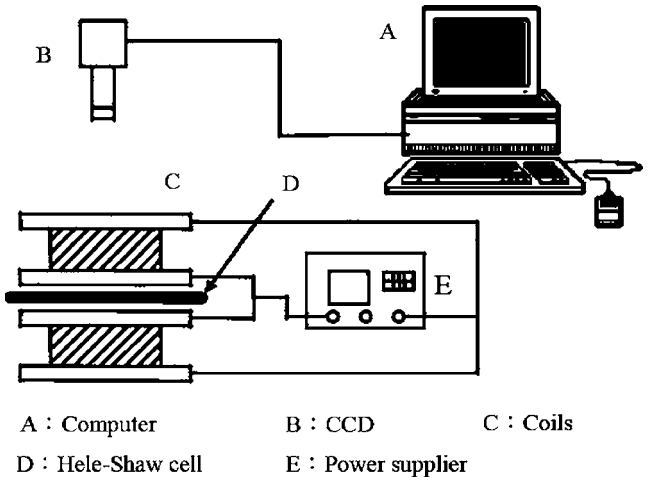

FIG. 1. Experimental apparatus consists of a miscible magnetic drop confined in a Hele-Shaw cell and subjected to a uniformed perpendicular field. The magnetic field is provided by a pair of coils in the Helmholtz configuration.

In this study, we present the first systematic experiments in miscible ferrofluids. Remarkable images of interfacial morphologies are demonstrated and further applied to clarify the dynamics of labyrinthine instability and to validate the theoretical and numerical findings that have been discussed intensively. In addition, the effects of gap widths to the mechanism of wave selection, which is well concluded in the conventional viscous fingering instability, can be also verified by the present experimental observations. The paper is organized as follows: After introducing the experimental setup in the next paragraph, results and discussion are presented in Sec. II. A qualitative description is first presented to identify the characteristic features and fingering structures. Subsequently, a more quantitative evaluation is presented. Section III presents concluding remarks.

B. Experimental apparatus

The experimental apparatus, as depicted in Fig. 1, consists of a magnetic drop with a diameter d surrounded by another fully miscible fluid and confined in a Hele-Shaw cell of two narrowly spaced flat plates. A uniform perpendicular field strength H is provided by a pair of coils in the Helmholtz configuration. The magnetic fluids used in the experiments are commercial light mineral oil based ferrofluids EMG905, produced by the Ferrotec Corp. The saturated magnetization of this particular ferrofluid is $M_s = 400$ G (or 400 mT). The viscosity (η_m) and density (ρ_m) of the ferrofluids are $\eta_m = 9 \times 10^{-3}$ N s/m^2 and $\rho_m = 1.24$ g/ml, respectively. Commercial light mineral oils with viscosity $\eta_0 = 2.7 \times 10^{-3}$ N s/m^2 and density $\rho_0 = 0.898$ g/ml are taken as the surrounding miscible fluids. The Hele-Shaw cell consists of two 10 mm thick parallel plates of plastic glasses. It has been confirmed that the fingerings depend significantly on the initial concentration gradients of the mixing interface.[17] In order to maximize the instability, a concentration jump of fully

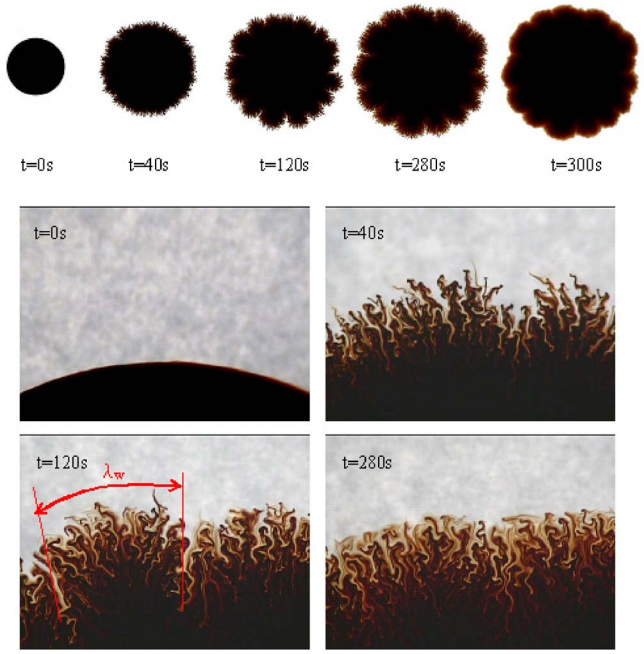

FIG. 2. (Color online) Sequential images of a drop with $d=24.6$ mm, $h=0.6$ mm, and $H=526$ Oe at $t=0,40,120,280$, and 300 s. Shown in the top row are overall images of the drop. The locally enlarged views are displayed in the bottom row. The external magnetic field is removed after $t=280$ s. Two interesting features of instability are observed: (i) numerous extremely fine fingering structures (labyrinthine fingers) and (ii) a nearly constant number of visible secondary waves.

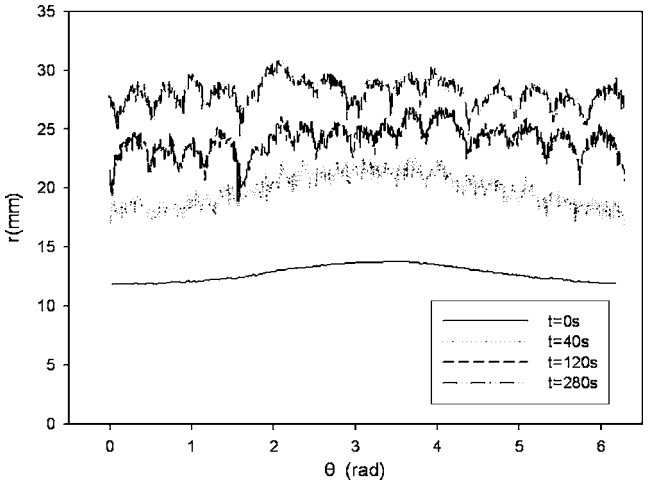

FIG. 3. Polar representations of the interfacial evolution for a drop with $d=24.6$ mm, $h=0.6$ mm, and $H=526$ Oe at $t=0,40,120$, and 280 s. The increasing radius r reflects an expanding area. The extremely irregular fluctuations and apparent wave behaviors represent pronounced labyrinthine fingers and secondary waves, respectively.

magnetized ferrofluids at the initial mixing front is desired. As a result, a mobile circular divider, whose top is closely sealed to the top plate, is initially placed at the center of the cell. The magnetic (nonmagnetic) fluids are then injected inside (outside) the divider to form the drop (the surrounding fluids). By this way, premixing of the fluids is prevented before experiments. The power source is turned on instantly at the desired strength for 20 s to fully premagnetize the ferrodrop before removal of the divider. Consequently, the mobile divider is suddenly retreated downward for a height of the gap width, so that its top lies on the same plane of the bottom plate to start experiments. We record the interfacial morphologies of the ferrodrop by a charge-coupled device (CCD) camera. The images are used to analyze the fingering phenomena both qualitatively and quantitatively.

II. RESULTS AND DISCUSSION

A. Qualitative analysis: Influences of field strengths and cell gap widths

The experimental results for a representative case with an initial diameter $d=24.6$ mm subjected to a field strength $H=526$ Oe in a cell gap width $h=0.6$ mm are presented first as the images shown in Fig. 2. We like to point out that the ferrodrop has almost reached its saturated strength of magnetization under this condition. Illustrated by these snapshots of morphological evolution, immediately after removal of the divider at $t=0$ s, the magnetic drop shows significant expansion associated with a great number of extremely fine fingering structures at $t=40$ s. While these fine fingers keep developing as time proceeds ($t\geq 120$ s), there are about 16 visible waves, we referred to as secondary waves herein, evolve in the interfacial region. Affected continuously by both the field induced dipolar force and the natural diffusion, all the characteristic features, including area expansion, development of fine fingering structures, and evolution of visible waves, remain significantly until the absence of the magnetic field after $t=280$ s. In addition, a constant number of secondary waves at $n\approx 16$ can be observed during the entire evolution. Unlike the immiscible situation, which the initial shape is restored by surface tension after removal of the field, reversal to a circular miscible drop is not possible. Once the field is absent, the dominant diffusive effects smooth off fine fingering structures rapidly, as shown at $t=300$ s. Distinguishable waves remain on the fringe with apparent dispersions. Figure 3 shows the curves by polar representations of interfacial evolution, in which all the characteristic features can be observed more clearly. The nearly flat curve of $r\approx 12.3$ mm at $t=0$ s represents a circular initial interface. Afterward, the increasing radius r reflects an expanding area. We would like to point out that an apparent area expansion of the drop is mainly caused by effects of diffusion and strong opaqueness of the ferrofluids. According to light inspection tests, the miscible fluids appear nearly opaque for a concentration of ferrofluids greater than 5%. As a result, the observing area of ferrodrop is significantly exaggerated compared to its actual area, which follows the conservation law of concentration. This is clearly demonstrated by expansion in the absence of a magnetic field ($H=0$ Oe) shown in Fig. 4. Besides the area expansion, polar representations also indicate the appearance of distinguishable waves associated with extremely irregular fluctuations for all the curves of $t\geq 40$ s. The irregular fluctuations and the apparent waves represent the fine fingering structures and the secondary waves, respectively. It is noteworthy that this pattern of

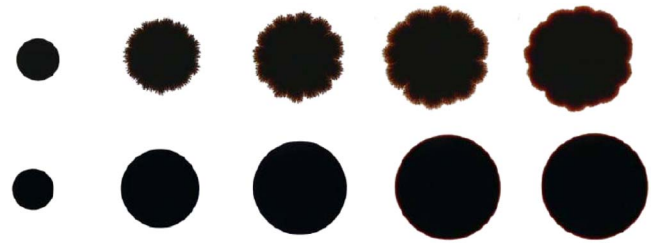

FIG. 4. Sequential snapshots of a drop with $d=24.6$ mm and $h=0.6$ mm at $t=0,40,120,280$, and 300 s (from left to right) for $H=187$ Oe (top row) and $H=0$ Oe (bottom row). The external magnetic field is removed after $t=280$ s. The labyrinthine fingers can be seen to be less pronounced for a weaker field strength.

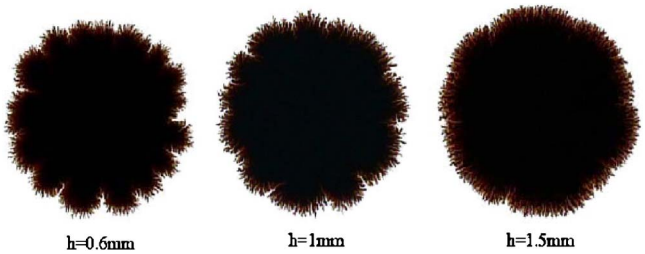

FIG. 5. Images of interfacial morphologies of drops with $d=24.6$ mm and $H=526$ Oe at $t=120$ s for various gap widths $h=0.6,1$, and 1.5 mm. The secondary wave numbers n depend strongly on the gap widths, and are counted at about $n\approx 16,12$, and 8 for the gap widths $h=0.6,1$, and 1.5 mm, respectively.

interfacial instability resembles the corresponding simulation based on the Hele-Shaw model with similar control parameters by Wen *et al.*[20] at an early time period $t\leq 40$ s. Nevertheless, qualitative discrepancy occurs at a later time stage $t\geq 40$ s when the secondary waves are formed. The formation of secondary waves is not observed in simulations.[16,18,19] This discrepancy confirms the inability of the Hele-Shaw model to completely capture the unstable modes reported in conventional viscous fingering studies[22–27] as well as the theoretical results in ferrofluids.[17] Further discussion regarding the secondary waves is presented in latter paragraphs. According to the evolution described above, two interesting features of instability are observed: (i) numerous extremely fine and irregular fingering structures and (ii) a nearly constant number of visible secondary waves. More detailed discussions of these two features are presented in the following.

We first focus on discussion of the extremely fine fingering structures, which are triggered by the magnetic dipolar forces and referred to as labyrinthine fingers herein. It is noteworthy that miscible labyrinthine fingers show uniquely qualitative features compared to the immiscible labyrinthine fingers or the conventional viscous fingers. Lacking the constraint by surface tension, the formation of miscible labyrinthine fingers is much more irregular with sharper fingertips than their immiscible counterparts, as shown by the enlarged images in Fig. 2. In addition, triggered by the magnetic forces, these miscible labyrinthine fingers grow outward from $t=40$ s to $t=280$ s without apparent shielding effects that are commonly seen in the conventional viscous fingerings. Another feature that characterizes the miscible labyrinthine fingers is the rare finger merging behavior, which results from mutual expelling between the magnetized fingers. Nevertheless, the local concentration of magnetic fluid is decreased because of mixings. Consequently, the prominence of miscible labyrinthine fingers is weakened and leads to more significant mixing around the circumferential region. The weaker labyrinthine fingerings can be identified by the lighter color within individual fingers at the later time $t=280$ s. In general, the miscible labyrinthine fingers observed in the experiments qualitatively resemble the predictions by relevant numerical simulations based on an augmented Hele-Shaw model[16,20] in which the effects of magneto-potential are included. The great similarities between the experiments and simulations, especially at an early time period $t\leq 40$ s before the appearances of secondary waves, suggest the applicability of the conventional Hele-Shaw model to qualitatively predict fine labyrinthine fingers, which are dominated by magnetic dipolar forces.

Early studies of immiscible situations have concluded that these labyrinthine fingers depend strongly on strengths of the external fields H and the cell gap widths h.[1,4–13] Similar results have also been reported in theoretical miscible investigations.[16–19] Here, we perform systematically miscible experiments, by varying H and h, in order to validate these theoretical predictions. Representative results of the interfacial evolution for a weaker field strength ($H=187$ Oe) and a zero field strength ($H=0$ Oe) are displayed in Fig. 4. Compared to the results of a stronger field strength $H=526$ Oe at the same times shown in Fig. 2, a weaker magnetic field $H=187$ Oe leads to slightly stronger dispersive effects which can be identified by a larger area of lighter color around the circumferential region. The labyrinthine fingers are seen to be less pronounced. In addition, formation of the secondary waves is less apparent as well. Even though the influences are not easy to be distinguished qualitatively by the images, a more distinct quantitative comparison shown in the next section confirms the above observations. For the case of a purely diffusive drop $H=0$ Oe, a circular front is nicely preserved without interfacial instability. These observations give qualitative confirmations that more intensively fingering instabilities result from stronger field strengths. Another parameter that affects the labyrinthine fingers is the gap width h. It had been clearly concluded from immiscible investigations that wider gap widths would result in stronger magneto-potentials and thus lead to more intensive labyrinthine fingers. Typical results for three gap widths $h=0.6,1.0$ and 1.5 mm at the same time, $t=120$ s, are shown in Fig. 5. Due to the extremely fine and irregular structures, no apparently distinguishable influence to the labyrinthine fingers can be concluded just by determining their overall morphologies. Nevertheless, the quantitative evaluations presented in the next section will give a clear conclusion. On the other hand, significant effects of different gap widths to the numbers of secondary waves are found. More detailed discussions regarding the secondary waves are presented in the next paragraph.

We now explore the interesting feature of secondary waves appearing on the interfacial fringe. For the reference

cases with a field strength $H=526$ Oe shown in Fig. 2, the interfacial region of the miscible drop always shows a certain number of secondary waves. This secondary wave can also be identified in the enlarged image at $t=120$ s where the typical wavelength is denoted as λ_w. Associated with the overall drop expansion described in the above paragraph, the secondary waves also grow continuously as time proceeds. We like to point out that these secondary waves are induced by the local magnetic microconvection nearby the mixing front, which depends on the local concentration distribution.[17] As we mentioned earlier, in order to maximize the instability the magnetic drop is fully premagnetized before contacting the surrounding fluids, thus prevents any initial concentration smearing by diffusion. As a result, dependency of the initial concentration smearing time is excluded in the present study. It is also noteworthy that the number of secondary waves, denoted as n, remains nearly constant during the entire period before removal of the field. The growth and number of waves can also be identified by the curves in polar representation shown in Fig. 3, where the shapes of curves remain quite similar with a nearly constant wave number for all times. In order to quantitatively analyze the formation of secondary waves, the number of secondary waves is counted visually from the images and polar plots as $n\approx 16$. The influences of field strengths on the secondary waves can be observed by comparing Fig. 2 ($H=526$ Oe) and Fig. 4 ($H=187$ Oe) for a fixed gap width $h=0.6$ mm. It can be seen that the number of secondary waves n depends insignificantly on the field strengths if h is kept constant. For these two cases, the number of secondary waves remain closely at about $n\approx 16$ and 15 for $H=526$ Oe and 187 Oe, respectively. Similar results are also observed for other field strength conditions. On the other hand, the gap width strongly affects the number of secondary wave, as shown in Fig. 5. The wave numbers are counted at $n\approx 16, 12, 8$ for the gap widths $h=0.6, 1, 1.5$ mm. These observations lead to an important conclusion that formation of secondary waves is mainly determined by the gap width h rather than the field strength H. A more quantitative correlation of λ and h will be addressed in the next section. The above interesting finding is consistent with the situations of miscible viscous Saffman-Taylor instability.[22–26] In the Stokes regime, i.e., $\mathrm{Pe}, \mathrm{Ra} > O(10^2)$, the wavelength λ of miscible fingering instability is dominated by the third-dimensional effect. In the present situation of a flow driven by magnetic forces, the magnetic Peclet numbers are estimated to be at $\mathrm{Pe}\approx O(10^6)$ or $\mathrm{Pe}_h\approx O(10^4)$ if scaled by gap width h,[28,29] which well satisfies the condition of the Stokes regime. As a result, even with different driving mechanisms it is expected that the secondary waves of present magnetically driven flow should be similarly dominated by the gap width. The above results suggest an important implication regarding the appropriateness of the Hele-Shaw model, which is commonly adopted for the numerical simulations.[16,18–20] Since the occurrences of extremely fine labyrinthine fingers are triggered by magnetic polar forces, the augmented Hele-Shaw model, which includes the magneto-potential effects, is able to reproduce the labyrinthine fingers. However, formation of secondary waves is gap dominated in the Stokes regime, and it cannot be accurately simulated by the Hele-Shaw equations. As a result, special caution is needed when applying the Hele-Shaw model for simulations of miscible magnetic fluids.

B. Quantitative analysis: Wave numbers and mixing interfacial lengths

Based on the results discussed in the previous section, two important qualitative findings are concluded: (i) the wave number n of secondary waves is predominated by the third dimension h; (ii) the field strength H mainly affects the prominence of the labyrinthine fingers. The purposes of this section are to evaluate these effects in a more quantitative way.

In order to further verify the dependence of wave number n of secondary waves and gap width h, experiments with various combinations of initial diameters $d=24.6$ and 14.76 mm under field strengths $H=526$, 366, and 187 Oe are carried for three gap widths of $h=0.6$, 1, and 1.5 mm. The mean values of wave numbers are plotted versus gap widths in Fig. 6. For conditions with the same initial sizes, it is clear that the wave number n is mainly dependent on the gap width h. The influence of field strength H is insignificant to the number of waves. A nearly inverse proportionality of the wave number n to the gap width h is also observed for a constant initial diameter, i.e., $d=24.6$ mm. As the effects of initial diameters, a larger initial size provides a longer circumference to form secondary waves, so that a higher wave number is observed in a larger initial diameter for a fixed gap width such as $d=24.6$ and 14.76 mm at $h=0.6$ mm, as shown in Fig. 6. As described in previous paragraphs, strong dependence of nearly linear correlations between wave numbers (or wavelength) and gap widths has been reported in various flow situations, which are similar to the present study. In order to quantify the dependence, we define a characteristic wavelength λ as $\lambda\equiv\pi d/n$, and corresponding wavelengths versus gap widths are plotted in Fig. 7. For all the experimental situations, wavelengths and gap widths closely follow a correlation of $\lambda\approx(7\pm1)h$. This correlation is in the same trend as the results obtained in the viscous fingering situations.[22–25]

The quantitative evaluation for prominence of miscible labyrinthine fingers can be analyzed by the mixing interfacial length.[16,18,19,30] We calculate the normalized mixing interfacial lengths L defined as

$$L(t)=\frac{1}{L_0(t)}\int_S\sqrt{\left(\frac{\partial c}{\partial x}\right)^2+\left(\frac{\partial c}{\partial y}\right)^2}\,dxdy,$$

where c is the concentration of magnetic fluid and S is the experimental domain. $L_0(t)$ represents the mixing interfacial length under zero magnetic field strength. In general, the interfacial length starts to increase once the fingering instability is triggered, so an earlier growth or a higher growth rate of interfacial length represents more vigorous labyrinthine fingerings.[16,18,19] To obtain concentration distributions for calculations, the experimental images are scanned and read into the Matlab software. Subsequently, the strengths of hues are converted into the corresponding values of concentration. The mixing interfacial lengths are calculated accord-

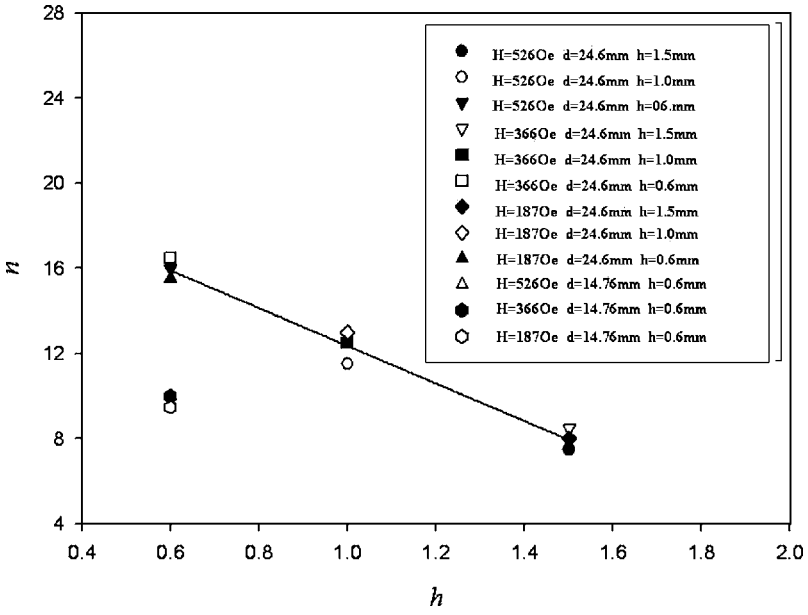

FIG. 6. The number of secondary waves n versus gap width h. The wave numbers are mainly dependent on the gap widths and initial diameters but not field strengths. A nearly inverse proportionality of wave number n to gap width h for a fixed initial diameter, i.e., $d=24.6$ mm, can also be observed.

ingly. We should note the inability to identify whole range of concentration distribution due to strong opaqueness of magnetic fluids, exact calculations of mixing interfacial lengths are not possible. Nevertheless, accurate estimations are obtained by these approximated concentration fields in the cases of zero field strengths, where the drops remain quite circular as demonstrated in Fig. 4. As a result, all the estimated interfacial lengths, which are based on the same scanned conditions, can be applied for quantitative comparisons between various situations. These estimated interfacial lengths L for different values of H and h are shown in Fig. 8. All the mixing interfacial lengths show rapid growths before reaching nearly asymptotic values. These evolving trends agree well with the numerical simulations.[16,20] Once the fields are removed after ($t \geq 300$ s), all the interfacial lengths collapse to near unity, which represent situations of pure diffusion without magnetic effects, by the strong dispersion. In addition, the most significant growth, represented by an earliest onset time, a largest growth rate and a longest interfacial length, occurs at the condition of a strongest field strength $G=526$ Oe and a widest gap width $h=1$ mm. Correspondingly, a weaker strength $G=187$ Oe and a narrower width $h=0.6$ mm results in a least growth of interfacial length. The quantitative comparisons confirm more vigorously labyrinthine fingerings at either a wider gap h or a stronger field strength H, which validate the early theoretical and numerical results.[16–19]

To conclude the discussion, we like to address a very relevant and important result by a recent theoretical study in miscible magnetic fluids.[17] In this study, linear stability analysis is carried for a sharp and a diffused interface, respectively. Growth rates for various wave numbers k are obtained as a function of a dimensionless parameter Cm defined as the ratio of diffusive time to magnetic-induced

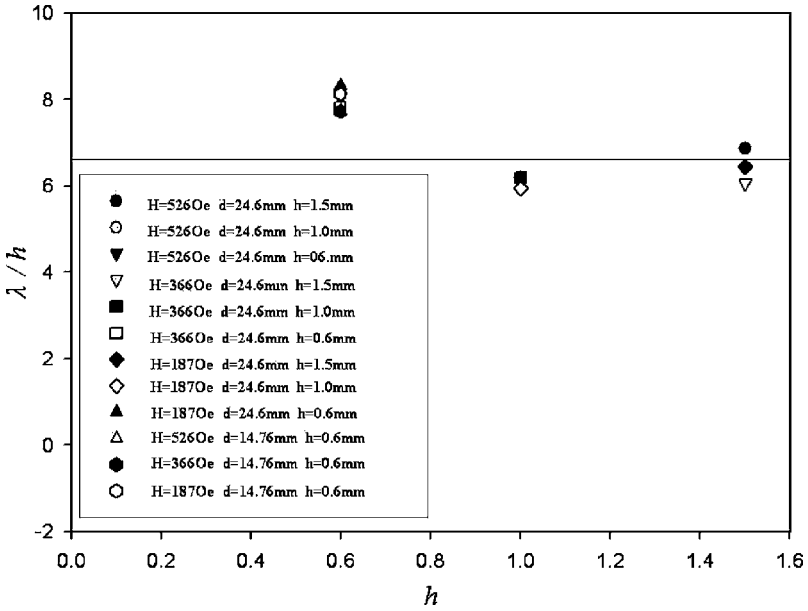

FIG. 7. For all the situations experimented, the wavelengths λ and gap widths h closely follow a correlation of $\lambda \approx (7 \pm 1)h$.

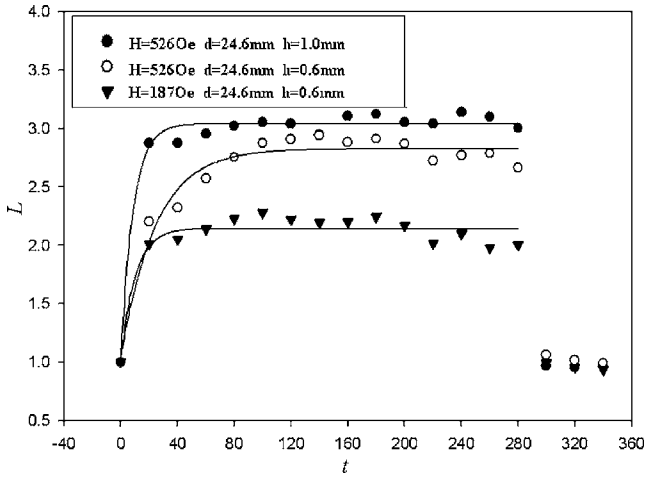

FIG. 8. Evolutions of normalized interfacial lengths L for various parameters; it is quantitatively confirmed that more intensively labyrinthine fingers are triggered either for stronger field strengths or wider gap widths.

convective time, which is an equivalent of Peclet number (Pe) to the present situation. The theoretical investigation for a sharp interface, that is similar to the present experimental condition, obtains a critical value of $Cm_{cr}=5.572$ to lose stability at a wave number of $k_{cr}=5.343$. It would be desired if a direct correlation between these theoretical results and the present experiments could be established. Nevertheless, the analysis is carried for a relatively low value of $Cm \leq O(10)$ based on the Darcy formulation, which the effects of gap widths might not be significant as discussed above. On the other hand, wave numbers, growth rates and the most dangerous modes in a diffused interface are predicted both based on the Darcy and the Brinkman formulations as functions of initial diffusion times for an asymptotic value $Cm \rightarrow \infty$. Nevertheless, besides the different initial condition of a diffused interface, two distinct instabilities are observed in the present experiments. It is unclear whether the wave numbers predicted represent the modes of magnetic-dominated labyrinthine fingers or secondary waves that depend on the gap effects. As a result, further studies would be necessary to clarify the correct representation of these theoretical results.

III. CONCLUSION

We present the first complete experimental study on the interfacial instability of miscible magnetic fluids in a Hele-Shaw cell under a uniform and perpendicular field. Vigorous interfacial instabilities are experimentally observed. Two distinct features of instabilities can be classified: (i) the miscible labyrinthine fingers caused by magnetic dipolar forces; (ii) the secondary waves dominated by third-dimensional effects. Due to the lack of constraint by surface tension, the formation of miscible labyrinthine fingers is much more irregular with sharper fingertips than their immiscible counterparts. These labyrinthine fingers qualitatively validate the predictions by relevant numerical simulations.[16,20] In addition, quantitative comparisons of interfacial lengths confirm that the prominence of labyrinthine fingers is mostly affected by both magnetic field strengths and gap widths. On the other hand, selections of the secondary wavelengths are mainly dominated by gap widths and depend insignificantly on field strengths. Influenced continuously by magnetic dipolar forces and diffusive effects, these secondary waves continue to expand with a nearly constant number of waves. The characteristic wavelengths λ of secondary waves can be approximated as $\lambda \approx (7 \pm 1)h$, which are consistent with earlier findings on the viscous fingering instabilities.[22–26] These results also confirm the inability of the augmented Hele-Shaw model to accurately portray the formation of secondary waves, which are dominated by gap effects in a Stokes regime [$\mathrm{Pe} > O(10^2)$]. However, the Hele-Shaw model, which includes the magneto-potential effects, is well able to reproduce the labyrinthine fingers.

ACKNOWLEDGMENT

C.-Y.C. thanks the National Science Council of the Republic of China for financial support through Grant No. NSC 94-2212-E-224-011.

[1] R. Rosensweig, *Ferrohydrodynamics* (Cambridge University Press, Cambridge, 1985).
[2] E. Blums, A. Cebers, and M. M. Maiorov, *Magnetic Fluids* (de Gruyter, New York, 1997).
[3] C.-Y. Chen, S.-Y. Wu, and J. Miranda, "Fingering patterns in the lifting flow of a confined miscible ferrofluid," Phys. Rev. E **75**, 036310 (2007).
[4] A. Cebers and M. Maiorov, "Magnetostatic instabilities in plane layers of magnetizable liquids," Magnetohydrodynamics (N.Y.) **16**, 21 (1980).
[5] A. Cebers and M. Maiorov, "Structures of interface of a bubble and magnetic fluid in a field," Magnetohydrodynamics (N.Y.) **16**, 231 (1980).
[6] S. Langer, R. Goldstein, and D. Jackson, "Dynamics of labyrinthine pattern formation in magnetic fluids," Phys. Rev. A **46**, 4894 (1992).
[7] A. Dickstein, S. Erramilli, R. Goldstein, D. Jackson, and S. Langer, "Labyrinthine pattern formation in magnetic fluids," Science **261**, 1012 (1993).
[8] D. Jackson, R. Goldstein, and A. Cebers, "Hydrodynamics of fingering instabilities in dipolar fluids," Phys. Rev. E **50**, 298 (1994).
[9] A. Cebers, "Stabilities of diffusion fronts of magnetic particles in porous media (Hele-Shaw cell) under the action of external magnetic field," Magnetohydrodynamics (N.Y.) **33**, 48 (1997).
[10] A. Cebers and I. Drikis, "Labyrinthine pattern formation in magnetic liquids," *Free Boundary Problems: Theory and Applications*, edited by Athanasopoulos *et al.* (Chapman and Hall/CRC, New York, 1998).
[11] C. Flament, G. Pacitto, J. Bacri, I. Drikis, and A. Cebers, "Viscous fingering in a magnetic fluid. I. Radial Hele-Shaw flow," Phys. Fluids **10**, 2464 (1998).
[12] I. Drikis and A. Cebers, "Viscous fingering in magnetic fluids: numerical simulation of radial Hele-Shaw flow," J. Magn. Magn. Mater. **201**, 339 (1999).
[13] G. Pacitto, C. Flament, and J. Bacri, "Viscous fingering in a magnetic fluid. II. Linear Hele-Shaw flow," Phys. Fluids **13**, 3196 (2001).
[14] C.-Y. Wen, C.-Y. Chen, C.-H. Tsai, and D.-C. Kuan, "Labyrinthine instabilities of a magnetic droplet in a Hele-Shaw cell," Magnetohydrodynamics **41**, 215 (2005).
[15] M. M. Maiorov and A. Cebers, "Magnetic microconvection on the diffusion front of the ferroparticles," Magnetohydrodynamics (N.Y.) **19**, 376 (1983).
[16] C.-Y. Chen, "Numerical simulations of fingering instabilities in miscible magnetic fluids in a Hele-Shaw cell and the effects of Korteweg stresses," Phys. Fluids **15**, 1086 (2003).
[17] A. Igonin and A. Cebers, "Labyrinthine instability of miscible magnetic fluids," Phys. Fluids **15**, 1734 (2003).
[18] C.-Y. Chen, H.-J. Wu, and L. Hsu, "Numerical simulations of labyrinthine instabilities on a miscible elliptical magnetic droplet," J. Magn. Magn. Mater. **289C**, 365 (2005).
[19] C.-Y. Chen and H.-J. Wu, "Numerical simulations of interfacial instabilities on a rotating miscible magnetic droplet with effects of Korteweg stresses," Phys. Fluids **17**, 042101 (2005).

[20]C.-Y. Wen, C.-Y. Chen, D.-C. Kuan, and S.-Y. Wu, "Labyrinthine instability of a miscible magnetic drop," J. Magn. Magn. Mater. **310**, 1017 (2007).
[21]A. Mezulis and E. Blums, "On the microconvective instability in optically induced gratings," Phys. Fluids **18**, 107101 (2006).
[22]L. Paterson, "Fingering with miscible fluids in a Hele-Shaw cell," Phys. Fluids **28**, 26 (1985).
[23]E. Lajeunesse, J. Martin, N. Rakotomalala, and D. Salin, "3D instabilities of miscible displacements in a Hele-Shaw cell," Phys. Rev. Lett. **79**, 5254 (1997).
[24]J. Fernandez, P. Kurowski, L. Limat, and P. Petitjeans, "Wavelength selection of fingering instability inside Hele-Shaw cells," Phys. Fluids **13**, 3120 (2001).
[25]J. Fernandez, P. Kurowski, P. Petitjeans, and E. Meiburg, "Density-driven unstable flows of miscible fluids in a Hele-Shaw cell," J. Fluid Mech. **451**, 239 (2002).
[26]F. Graf, E. Meiburg, and C. Hartel, "Density-driven instability of miscible fluids in a Hele-Shaw cell: Linear analysis of the three-dimensional Stokes equations," J. Fluid Mech. **451**, 261 (2002).
[27]N. Goyal, H. Pichler, and E. Meiburg, "Variable-density miscible displacements in a vertical Hele-Shaw cell: Linear stability," J. Fluid Mech. **584**, 357 (2007).
[28]C.-Y. Chen, C.-H. Chen, and J. Miranda, "Numerical study of miscible fingering in a time-dependent gap Hele-Shaw cell," Phys. Rev. E **71**, 056304 (2005).
[29]C.-Y. Chen, C.-H. Chen, and J. Miranda, "Numerical study of pattern formation in miscible rotating Hele-Shaw flows," Phys. Rev. E **73**, 046306 (2006).
[30]C.-Y. Chen and E. Meiburg, "Miscible porous media flows in the quarter five-spot configuration. Part 1: The homogeneous case," J. Fluid Mech. **371**, 2233 (1998).